Science of the Total Environment 481 (2014) 522–532

Contents lists available at ScienceDirect

Science of the Total Environment

journal homepage: www.elsevier.com/locate/scitotenv

Inorganic aerosols responses to emission changes in Yangtze River Delta, China

Xinyi Dong [a], Juan Li [b], Joshua S. Fu [a,*], Yang Gao [a,c], Kan Huang [a], Guoshun Zhuang [d]

[a] Department of Civil and Environmental Engineering, The University of Tennessee, Knoxville, TN 37996, USA
[b] Shanghai Environmental Monitoring Center, Shanghai 200030, China
[c] Atmospheric Science and Global Change Division, Pacific Northwest National Laboratory, Richland, WA 99354, USA
[d] Center for Atmospheric Chemistry Study, Department of Environmental Science and Engineering, Fudan University, Shanghai 200433, China

HIGHLIGHTS

- Inorganic aerosols' seasonality and contribution for $PM_{2.5}$ are examined over YRD.
- Nighttime hydrolysis of N_2O_5 was demonstrated to be responsible for nitrate enhancement over YRD for all seasons.
- Nitrate mass concentration might be increased under NOx emission reduction in winter over YRD.

ARTICLE INFO

Article history:
Received 20 June 2013
Received in revised form 12 February 2014
Accepted 15 February 2014
Available online 12 March 2014

Keywords:
$PM_{2.5}$
YRD
Inorganic aerosols sensitivity

ABSTRACT

The new Chinese National Ambient Air Quality standards (CH-NAAQS) published on Feb. 29th, 2012 listed $PM_{2.5}$ as criteria pollutant for the very first time. In order to probe into $PM_{2.5}$ pollution over Yangtze River Delta, the integrated MM5/CMAQ modeling system is applied for a full year simulation to examine the $PM_{2.5}$ concentration and seasonality, and also the inorganic aerosols responses to precursor emission changes. Total $PM_{2.5}$ concentration over YRD was found to have strong seasonal variation with higher values in winter months (up to 89.9 μg/m^3 in January) and lower values in summer months (down to 28.8 μg/m^3 in July). Inorganic aerosols were found to have substantial contribution to $PM_{2.5}$ over YRD, ranging from 37.1% in November to 52.8% in May. Nocturnal production of nitrate (NO_3^-) through heterogeneous hydrolysis of N_2O_5 was found significantly contribute to high NO_3^- concentration throughout the year. In winter, NO_3^- was found to increase under nitrogen oxides (NOx) emission reduction due to higher production of N_2O_5 from the excessive ozone (O_3) introduced by attenuated titration, which further lead to increase of ammonium (NH_4^+) and sulfate (SO_4^{2-}), while other seasons showed decrease response of NO_3^-. Sensitivity responses of NO_3^- under anthropogenic VOC emission reduction was examined and demonstrated that in urban areas over YRD, NO_3^- formation was actually more sensitive to VOC than NOx due to the O_3-involved nighttime chemistry of N_2O_5, while a reduction of NOx emission may have counter-intuitive effect by increasing concentrations of inorganic aerosols.

1. Introduction

Fine aerosols ($PM_{2.5}$) has been listed as one of the criteria air pollutants in National Ambient Air Quality Standard (NAAQS) and thoroughly investigated in United States due to its adverse effects on public health, reduction of visibility, and also climate forcing in the past decade. Although the knowledge about $PM_{2.5}$ in China is limited due to relative less emphasis (Chan and Yao, 2008), the necessity of understanding $PM_{2.5}$ is well recognized recently. On Feb. 29, 2012, The Chinese Ministry of Environmental Protection (MEP) published the new China National Ambient Air Quality Standard (CH-NAAQS) in which $PM_{2.5}$ was announced as criteria pollutant for the very first time. Although both the annual (35 μg/m^3) and daily (75 μg/m^3) standards configured within CH-NAAQS are less strict compared with the US-NAAQS (15 μg/m^3 and 35 μg/m^3 for annual and daily standard, respectively), the significantly increased news reports about $PM_{2.5}$ thereafter implied the strong public interest in this issue. Especially, the national wide haze engulfed a large portion of Eastern China during the past winter promoted the important urgency for more efforts dedicated to understand $PM_{2.5}$ pollution. China National Environmental Monitoring Centre (CNEMC) reported monitored monthly average $PM_{2.5}$ for 74 major cities was 130 μg/m^3 and 85 μg/m^3 for January and February 2013, respectively (CNEMC, 2013), while the observed maximum daily average values were 766 μg/m^3 and 232 μg/m^3 for the two months, which substantially exceeded the CH-NAAQS.

* Corresponding author. Tel.: +1 865 974 2629; fax: +1 865 974 2669.
E-mail address: jsfu@utk.edu (J.S. Fu).

http://dx.doi.org/10.1016/j.scitotenv.2014.02.076
0048-9697/

Several pilot studies have already been performed with observational or modeling method to probe into $PM_{2.5}$ pollution over China from different perspectives. Streets et al. (2007) assessed local anthropogenic emission contribution to particles formation and reported observed daily average $PM_{2.5}$ ranged from 75 to 145 μg/m^3 in Beijing; Fu et al. (2010) examined pollution event driven by dust storm in Shanghai based on observations and reported 383 μg/m^3 $PM_{2.5}$ in April 2007; Fu et al. (2012b) investigated biomass burning impacts from southeast Asia with modeling method and reported long-range transport could contribute to 64 μg/m^3 over Eastern Asia. A couple of pioneering studies conducted recently also provide more detailed information about $PM_{2.5}$ speciation over China. Huang et al. (2012) examined the composition measurements of $PM_{2.5}$ in Shanghai, and reported inorganic aerosols (nitrate (NO_3^-), sulfate (SO_4^{2-}), ammonium (NH_4^+)) could contribute up to 77% (48.86 ± 5.01 μg/m^3) of total $PM_{2.5}$ in typical pollution episodes, of which nitrate/sulfate ratio was also found to increase from 0.43 in 2000 to 0.75 in 2009. Pathak et al. (2011) reported observed exceptionally high concentrations of nitrate up to 42 μg/m^3 in Beijing and Shanghai, and concluded the high level summer time nitrate was due to hydrolysis of N_2O_5 based on box model simulation. Zhao et al. (2013a,b) reviewed the impacts of anthropogenic emission changes in China and reported up to 4.22 μg/m^3 of $PM_{2.5}$ deduction due to NOx and SO_2 emission reduction.

The above studies mainly focused on special air pollution episodes, while few of them have been performed to provide comprehensive examination of $PM_{2.5}$ pollution regarding its formation schemes, seasonality, and spatial distribution over China. Although studies applying box model described the essential inorganic aerosol chemistry mechanism, it can only represent some domain-averaged chemistry instead of distinguishing different chemical regimes. Fundamental uncertainties still exist due to the essential assumptions employed by box model such as stagnant conditions and aloft carry-over of air pollutants. Pathak et al. (2011) assumed a fixed ratio for NO_2/NOy and a linear relationship between nitric acid (HNO_3) and nitrogen dioxide (NO_2) to predict nitrate formation, while a steady-state might hardly be reached with intensive emission and rapid convection. More importantly, only a few studies have been documented to examine $PM_{2.5}$ responses to precursor emission changes over China. So in this paper, we applied MM5/CMAQ modeling system for a full year simulation to examine the seasonal variations of $PM_{2.5}$ over Yangtze River Delta (YRD). Anthropogenic emission control scenarios were also employed to investigate the sensitivity responses of inorganic aerosols to precursor emission changes. YRD was selected as the research area because it is one of the most important commercial and industrial center within China, and also a highly populated region with more than 80 million residences, of which 50 million are urban. Model description and evaluation was provided in Section 2. Section 3 discussed the seasonality of $PM_{2.5}$, and the inorganic aerosol responses in different seasons under predefined NOx and VOC emission control scenarios. Section 4 draws conclusions and summarizes major challenges and future prospects.

2. Materials and methods

2.1. Model description and simulation design

Community Multiscale Air Quality (CMAQ) modeling system developed by the US EPA (Byun and Schere, 2006) was selected to conduct simulations in this study. CMAQ has been widely applied to predict air pollutions over China in different studies and demonstrated its reliability (Fu et al., 2012b, 2013; Streets et al., 2007; Wang et al., 2014). In this study, CMAQ v4.6 was configured with 19 vertical layers extending from ground surface to 100mb with denser layers in lower atmosphere to better represent the mixing layer. There were three one-way nested modeling domains D1, D2, and D3 which mainly covered East Asia, eastern China, and YRD respectively, as shown in Fig. 1 (detailed model configuration is summarized in Table S1). We mainly focused on domain D3 which covered Shanghai, southern Jiangsu province and northern Zhejiang province with a 3 × 3 km grid resolution. Initial and boundary conditions for domain D1 was generated from GEOS-Chem global modeling results following the algorithm described in Lam and Fu (2009). Shanghai was selected as a representative city in this study to assess $PM_{2.5}$ pollution in typical urban areas within YRD. The meteorology filed was generated by the fifth-generation the National Center for Atmospheric Research (NCAR)/Penn State Mesoscale Model (MM5 version 3.3). Anthropogenic emission inputs for CMAQ modeling system was provided by the Intercontinental Chemical Transport Experiment-Phase B (INTEX-B) 2006 emission inventory (Zhang et al., 2009). Species include sulfur dioxide (SO_2), nitrogen oxides (NOx), carbon monoxide (CO), non-methane volatile organic compounds (NMVOC), PM_{10}, $PM_{2.5}$, black carbon aerosol (BC), organic carbon aerosol (OC), ammonia (NH_3), and methane (CH_4). NMVOC was categorized into 16 subspecies to match the CB05 chemical mechanism utilized in CMAQ (Yarwood et al., 2005). The 2D grid-cell emissions were obtained using top-down method (Du, 2008). Biogenic emissions were generated by the Model of Emissions of Gases and Aerosols from Nature (MEGAN) (Guenther et al., 2012).

Besides the baseline simulation, emission control simulations were also conducted in order to understand the sensitivity responses of

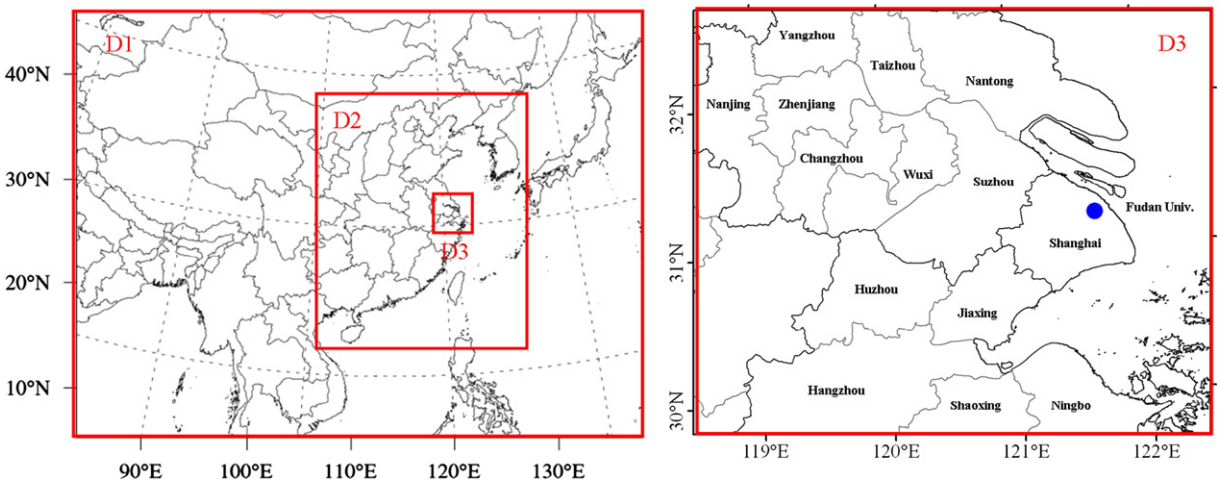

Fig. 1. Three one-way nested modeling domains at 27-km (East Asia: D1), 9-km (East China: D2), and 3-km (Yangtze River Delta: D3) resolutions. Blue cycle represents the observation site Fudan University.

$PM_{2.5}$ to precursor emission changes. Anthropogenic emissions in YRD region mainly comes from 4 sectors including industrial process (denoted as industry here and after), residential combustion (denoted as residential here and after), power plants, and transportation, which contribute 29%, 4%, 42%, and 25% of NOx emission respectively, and 39%, 29%, 5%, and 27% for VOC emission respectively. So five different sensitivity scenarios were defined based on emission species and sectors: 1) 20% NOx emission reduction from industry (I-N20) and 2) transportation (T-N20), 3). 20% VOC emission reduction from industry (I-V20) and 4) transportation (T-V20), and also 5) 85% NOx emission reduction from power plant (P-N85). These sensitivity scenarios are defined to investigate the different responses of $PM_{2.5}$ to emission changes from different sectors under different control percentages. All simulations were conducted following the monthly sequence with a 1-week spin-up period to minimize the influence of initial conditions.

2.2. Model evaluation

Validation of output meteorology filed from MM5 and output gaseous pollutants from CMAQ was reported in Dong et al. (2013). MM5 was demonstrated as capable of reproducing meteorology filed which agree well with surface observations.

Model evaluation for $PM_{2.5}$ and inorganic aerosols against surface measurements were conducted following the evaluation protocol proposed by the US EPA (EPA, 2007) by using key indicators including Normalized Mean Bias (NMB), Normalized Mean Error (NME), Mean Fractional Bias (MFB), Mean Fractional Error (MFE), and correlation coefficient as shown in Table 1. Modeling results from base simulation were compared with observations to conduct the evaluation. Observation site is described in the Supplementary material. For $PM_{2.5}$ evaluation, NMB, NME, MFB, and MFE values were −17.23%, 44.53%, −17.28%, and 50.25% respectively. While the benchmark suggested by the US EPA (EPA, 2007) were ±30% and 50% for MFB and MFE respectively, evaluation results for $PM_{2.5}$ indicated that model generally reproduce the ambient concentrations of fine particles well. Statistics summarized in Table 1 showed that model had moderate underestimations for NH_4^+ and NO_3^- and underestimated SO_4^{2-} with the largest discrepancy. As shown in Fig. 2, the Factor 2 (F2) analysis (Fu et al., 2012b) demonstrated that model simulated $PM_{2.5}$, NH_4^+ and NO_3^- has over 68%, 60%, and 76% fractions lie between 0.5 and 2.0 fold of the measurement data respectively, while the fraction for SO_4^{2-} was only 43% (time-series plots of model evaluation are summarized in Fig. S1 in the Supplementary material). CMAQ underestimation of SO_4^{2-} was probably due to the remained uncertainty of anthropogenic SO_2 emission of China.

Satellite retrieved Aerosol Optical Depth (AOD) product from MODerate Resolution Imaging Spectrometer (MODIS) instrument aboard the Terra satellite (Krotkov et al., 2008) was also used to evaluated CMAQ model performance. Terra achieved nadir view swath is usually around 10:30 local time, so AOD was calculated from CMAQ modeling results at 11:00 local time (CMAQ model time 03:00 UTC) following the approach described in Fu et al. (2012b). MODIS retrieved AOD was interpolated from 1° × 1° (latitude × longitude) to 27 km × 27 km in order to calculate model evaluation statistics, which was also summarized in Table 1 (spatial distribution plots comparing AOD from MODIS and CMAQ are summarized in Fig. S2). As shown in Table 1, CMAQ output demonstrated a very close spatial distribution pattern as MODIS observations, but underestimated AOD for all seasons, with NMB ranges from −61.14% in March, April, and May (MAM) to −30.95% in December, January, and February (DJF), indicating the satellite evaluation result was consistent with ground surface evaluation results. CMAQ underestimation of AOD may be attributed to reasons including: uncertainties of prediction of Secondary Organic Aerosol (SOA), exclusion of dust aerosol emission over northwestern China, and also the uncertainties of MODIS derived AOD.

In summary, the model could generally well reproduce the ambient concentrations and spatial distribution of fine particles over the research domain.

3. Results and discussion

3.1. Overview of $PM_{2.5}$ pollution over YRD

In this section, spatial distribution and seasonality of $PM_{2.5}$ in YRD were examined and evaluated according to the new published CH-NAAQS. Spatial distribution of annual average $PM_{2.5}$ concentration is shown in Fig. 3(a), which demonstrates that a large part of the research domain (58.2% of the grids within domain D3) is found to exceed the 35 μg/m^3 annual standard. The highest value is found in Nanjing as 132 μg/m^3. Almost all urban areas are found to have much higher $PM_{2.5}$ concentration than suburban and rural areas, indicating the particulate pollution might be more dependent on anthropogenic emission. $PM_{2.5}$ mass concentration also demonstrates a large seasonal variation. Fig. 3(b) describes the monthly averaged $PM_{2.5}$ concentrations in Shanghai (a 5 × 5 grid subsection from CMAQ modeling result is selected to represent the urban area of Shanghai here and after). Highest monthly $PM_{2.5}$ was occurred in January as 89.5 μg/m^3, and lowest value was occurred in July as 28.7 μg/m^3. Summer (June, July, and August (JJA)) generally has lower $PM_{2.5}$ than winter (DJF), which is probably due to higher planetary boundary layer (PBL) height and stronger advection and clean ocean air parcel introduced by Southeast Asia monsoon (SEAM). Winter time has more primary PM and precursors (SO_2, NOx) anthropogenic emissions due to intensified coal utilization for heating (Zhao et al., 2008). Model results also showed that there were 123 days in year 2006 that ambient $PM_{2.5}$ exceed the daily 75 μg/m^3 standard in Shanghai, indicating the serious pollution status within this region.

In order to understand the compositions of $PM_{2.5}$ over YRD, Fig. 3(b) also demonstrates the mass concentrations contributed by inorganic aerosols including SO_4^{2-}, NO_3^-, NH_4^+ (seasonal average nitrate, sulfate, and ammonium distributions was provided in Fig. S3), and other species (include BC, OC, sea-salt aerosol, and unspecified species) in Shanghai. Percentage contributions suggested that inorganic aerosols play an

Table 1
Model evaluation statistics for $PM_{2.5}$, SO_4^{2-}, NH_4^+, NO_3^-, and AOD.

Variables	Surface obs. evaluation				MODIS AOD evaluation			
	$PM_{2.5}$	SO_4^{2-}	NH_4^+	NO_3^-	DJF[1]	MAM	JJA	SON
Mean bias	−6.13 μg/m^3	−3.19 μg/m^3	−0.85 μg/m^3	−0.15 μg/m^3	−0.07	−0.21	−0.16	−0.08
Correlation	0.43	0.58	0.55	0.53	0.69	0.83	0.69	0.83
NMB (%)	−17.23	−51.12	−28.58	−8.66	−30.95	−61.14	−58.76	−37.82
NME (%)	44.52	55.92	49.88	74.91	43.78	61.14	60.41	42.35
MFB (%)	−17.28	−71.31	−35.61	21.74	−52.64	−97.76	−90.31	−57.11
MFE (%)	50.25	78.66	60.96	88.54	63.69	97.96	93.73	65.98
F2	0.68	0.43	0.60	0.76	–	–	–	–

[1] DJF: December, January, and February; MAM: March, April, and May; JJA: June, July, and August; SON: September, October, and November.

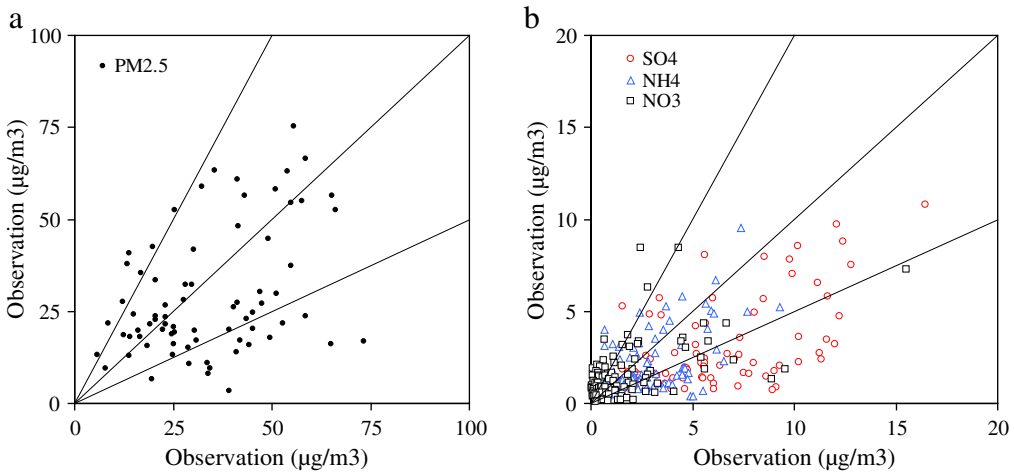

Fig. 2. F2 analysis for (a) total $PM_{2.5}$ and (b) SO_4^{2-} (red), NH_4^+ (blue), and NO_3^- (black).

important role. Total contributions of inorganic aerosols ranges from 37.1% (16.5 μg/m^3) in November to 52.8% (36 μg/m^3) in May. Inorganic aerosols also demonstrated strong seasonality as shown in Fig. 3(b). SO_4^{2-} was found to reach highest mass concentration as 17.3 μg/m^3 in January and lowest concentration as 6.6 μg/m^3 in July, NH_4^+ has largest value as 10.5 μg/m^3 in January and 2.8 μg/m^3 in July; maximum and minimum values for NO_3^- were 14.7 μg/m^3 and 1.3 μg/m^3 in March and July, respectively. Although NH_3 emission over YRD has strong seasonal variations and is most intensive from June to August (Wang et al., 2011), inorganic aerosols were found to have relatively lower mass concentrations in summer months than winter and spring.

Two indicators, Gas Ratio (GR; Ansari and Pandis, 1998) and Degree of Sulfate Neutralization (DSN; Pinder et al., 2008) are used to reveal the NH_3-rich or -poor status over YRD, with definitions shown as follows:

$$GR = \frac{([NH_3] + [NH_4^+]) - 2 \times [SO_4^{2-}]}{[NO_3^-] + [HNO_3]} \quad (1)$$

$$DSN = \frac{[NH_4^+] - [NO_3^-]}{[SO_4^{2-}]}. \quad (2)$$

GR < 0 indicates NH_3-poor condition, 0 < GR < 1 indicates NH_3-neutral, and GR > 1 indicates NH_3-rich condition. DSN < 2 indicates sulfate is insufficiently neutralized (NH_3-poor), and DSN > 2 indicates NH_3-rich condition. GR analysis is performed with CMAQ simulation results as shown in Fig. 4. All land area is found to have GR value greater than 1 in all seasons, indicating YRD area is NH_3-rich. DSN was calculated with surface observation data in Shanghai for March, April, August, November, and December, where the values were 8.7, 3.1, 22.8, 3.4, and 3.7 respectively. Both GR indicator based on modeling result and DSN indicator based on surface observations demonstrated that, majority part of YRD were identified as NH_3-rich throughout the entire year, which was also consistent with the finding from other study (Wang et al., 2011). So the relatively higher NH_3 emission and lower inorganic aerosols concentrations in summer indicated that seasonal variations of SO_4^{2-}, NO_3^-, and NH_4^+ might be more sensitive to emissions of SO_2 and NOx rather than NH_3, and the local meteorology condition may also play an important role by affecting both chemical and dispersion processes.

In addition, NO_3^- contribution to YRD was found much higher than values reported for other typical metropolitans. Babich et al. (2000) reported observed nitrate concentrations for 6 cities in the US, include: 3.1 μg/m^3 in Chicago, 2.1 μg/m^3 in Dallas, 3.6 μg/m^3 in Phoenix, 4.5 μg/m^3 in Riverside, 0.6 μg/m^3 in Philadelphia, and 0.2 μg/m^3 in Boston. Nitrate concentrations for rural sites were even lower over other regions. Malm et al. (2004) reported annual average nitrate concentration for the US based on 147 Interagency Monitoring of Protected Visual Environments (IMPROVE) observation sites, of which highest nitrate was found in southern California about 2.0 μg/m^3. While annual average NO_3^- was 7.06 μg/m^3 in our study, other studies also reported high NO_3^- concentration over YRD. Huang et al. (2012) reported NO_3^- in Shanghai was 6.3 ± 5.7 μg/m^3 in March based on ground surface observational data, Zhang et al. (2012) reported observed annual average NO_3^- in Jinsha (a suburban area within YRD region, about 130 km northward of Shanghai) was 7.2 μg/m^3 from 2006 to 2007. The high

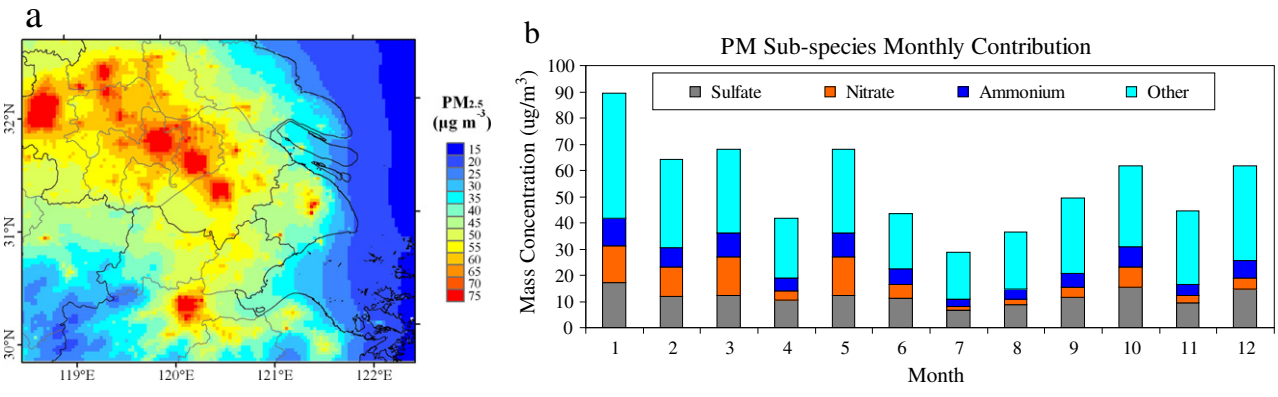

Fig. 3. (a) Spatial distribution of annual average $PM_{2.5}$ over YRD (b) inorganic aerosols contributions for each month in Shanghai.

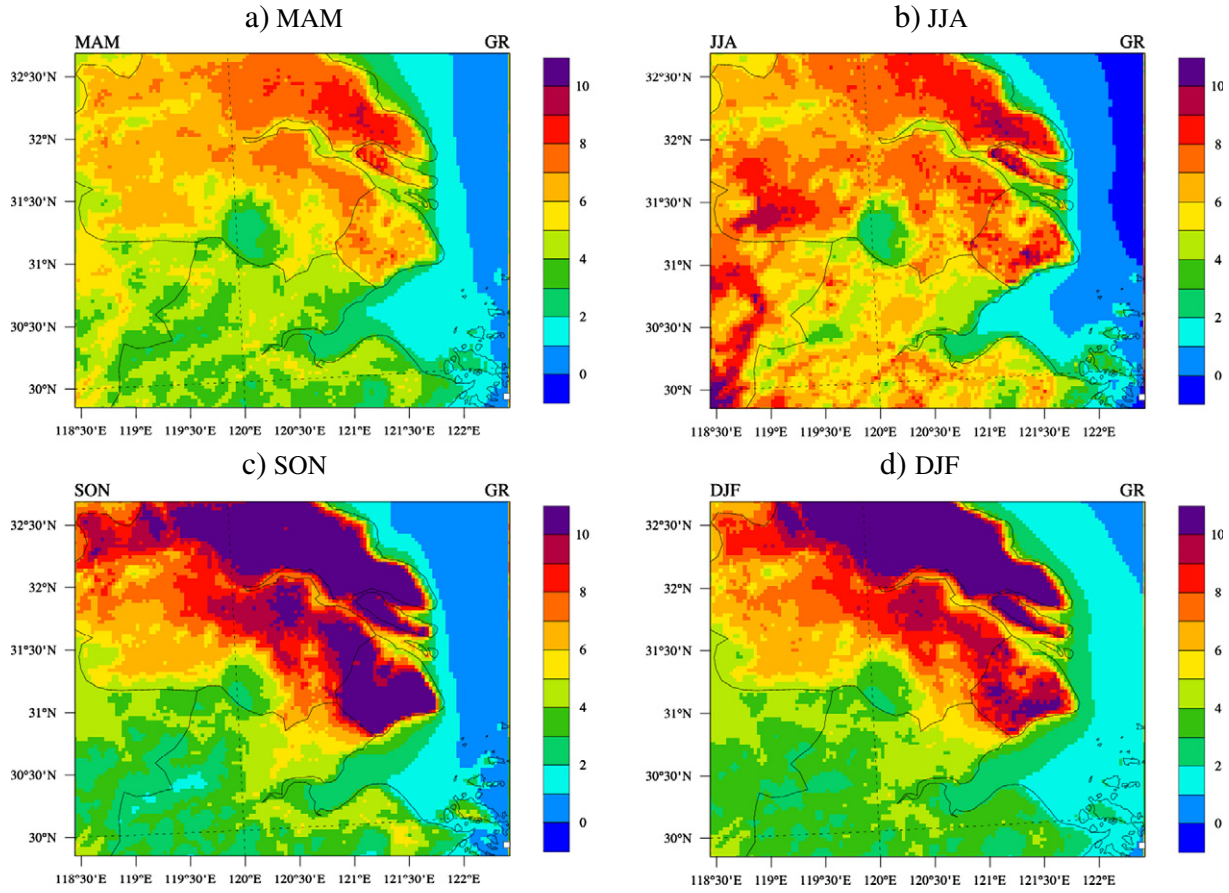

Fig. 4. Gas ratio (GR) analysis for (a) MAM, (b) JJA, (c) SON, and (d) DJF. GR values greater than 1.0 indicate NH_3-rich condition, within 0–1 indicate NH_3-neutral condition, and GR values less than 0 indicate NH_3-poor condition.

proportion of NO_3^- in YRD not only indicated its significant impact on ambient $PM_{2.5}$ concentration, but also implied an adverse effect on air quality by increasing the air and wet deposition acidity in the local area since the abundant nitrate probably implied a higher HNO_3 production rate (Zhao et al., 2008).

3.2. Nighttime enhancement of NO_3^- over YRD

In order to understand the high contribution of nitrate aerosol to total $PM_{2.5}$ over YRD, it is necessary to briefly summarize the chain reactions involved although the chemistry has been well documented. As an important precursor for both O_3 and NO_3^-, NOx may lead to formation of O_3, nitric acid (HNO_3), and NO_3^- through reactions (Yarwood et al., 2005):

$$NO_2 + h\nu \xrightarrow{O_2} O_3 + NO \quad \text{R1}$$

$$NO_2 + OH \rightarrow HNO_3. \quad \text{R2}$$

Reaction ($NO_2 + h\nu \rightarrow^{O_2} O_3 + NO$ R1) is one of the most important pathway for O_3 formation. Reaction (R2) is the major pathway for HNO_3 formation during daytime because of photochemical production with hydroxyl radicals. HNO_3 will further react with gas phase NH_3 though homogeneous reaction and form nitrate particles when water vapor is available.

Nocturnal production of nitrate consists of the following reactions:

$$NO + O_3 \rightarrow NO_2 + O_2 \quad \text{R3}$$

$$NO_2 + O_3 \rightarrow NO_3 \quad \text{R4}$$

$$NO_2 + NO_3 \rightarrow N_2O_5 \quad \text{R5}$$

$$N_2O_5 + H_2O \rightarrow 2HNO_3. \quad \text{R6}$$

The reactions (R3)–(R5) pathway dominates nitrate formation through nighttime instead of reaction (R2) mainly because OH is depleted and also the rapid photolysis of NO_3 ceases without after sunset, which favors the formation of N_2O_5. Production of N_2O_5 though reaction (R5) is especially favored under low temperature condition, and hydrolysis formation of HNO_3 through reaction (R6) is favored by high relative humidity.

It is important to notice that O_3 plays a key role to facilitate formation of NO_3^- through both reactions (R2) and (R3)–(R6) pathways. While NOx can produce O_3 in daytime and titrate O_3 in nighttime, formation of O_3 can also be initiated by the reactions of VOC with OH radical:

$$VOC + OH \xrightarrow{O_2} RO_2 + H_2O. \quad \text{R7}$$

And further completed by NO and VOC through chain productions:

$$RO2 + NO \xrightarrow{O_2} \text{secondary VOC} + HO_2 + NO_2 \quad \text{R8}$$

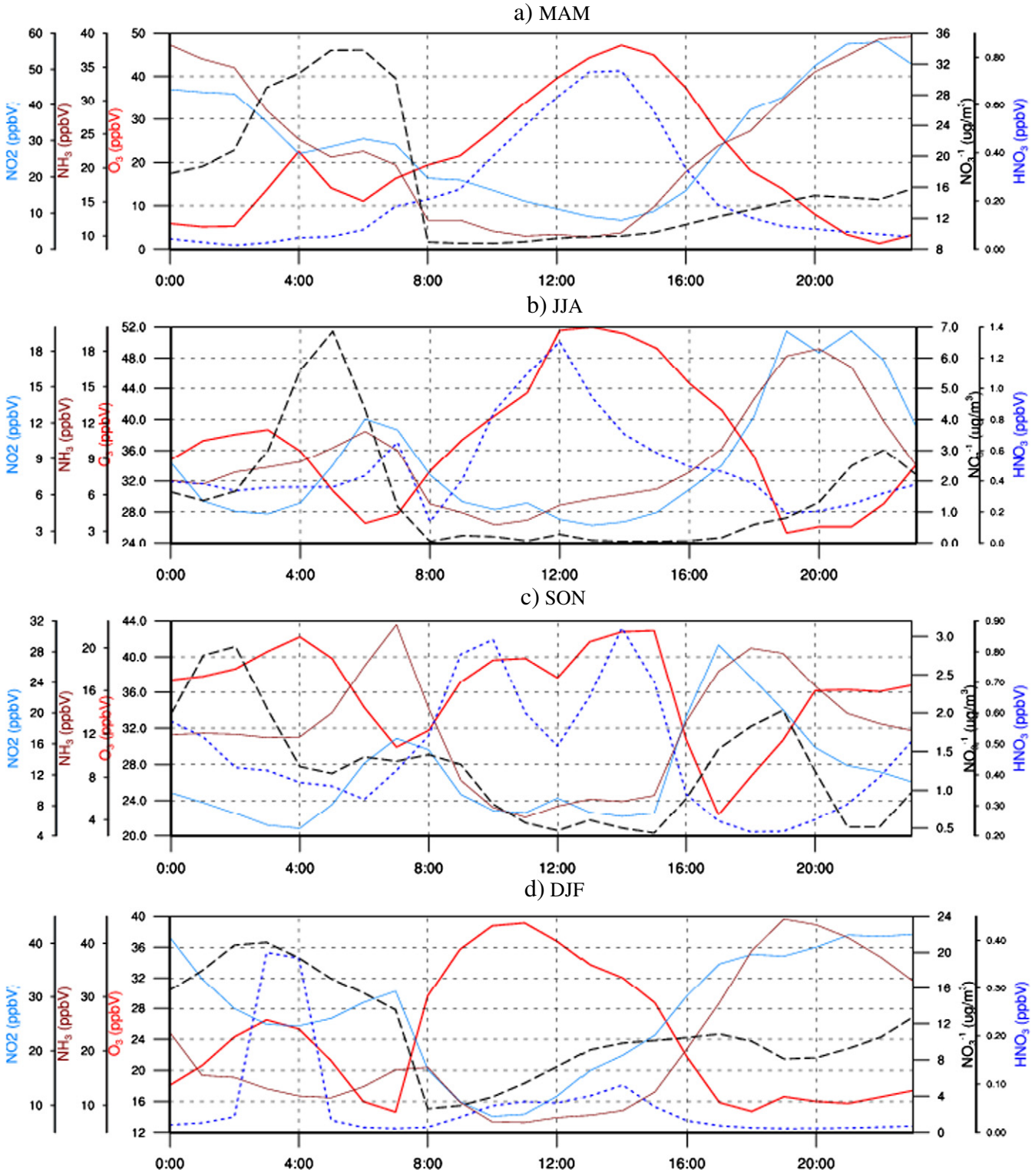

Fig. 5. Monthly average diurnal profiles of NO_2 (skyblue solid lines), NH_3 (brown solid lines), O_3 (red solid lines), NO_3^- (black dash lines), and HNO_3 (blue dash lines) for (a) MAM, (b) JJA, (c) SON, and (d) DJF.

$$HO_2 + NO \rightarrow OH + NO_2. \quad \text{R9}$$

In highly polluted areas with large NOx and NH_3 emissions, both daytime and nighttime formations of HNO_3 will lead to rapid production of NO_3^-. But nighttime enhancement of NO_3^- is likely to be more significant since photolysis reaction ($NO_2 + h\nu \rightarrow^{O_2} O_3 + NOR1$) serves as an important sink for NO_2 during daytime, while on the other hand, titration reaction (R3) provides a source for NO_2 during nighttime. While most anthropogenic emissions are usually released during daytime, the importance of nighttime enhancement of nitrate pollution has been revealed only in very few studies. Pun and Seigneur (2001) reported nighttime enhancement of NO_3^- in San Joaquin Valley based on box model simulations, and Pathak et al. (2011) reported summer

nocturnal accumulation of NO_3^- in Beijing and Shanghai also with box model. In our study however, the importance of nocturnal production of NO_3^- was demonstrated with 3D model simulation for the very first time. Moreover, rather than previous studies drawing conclusion based on a few days box model simulations, our simulation found that the nitrate enhancement could happen in all seasons.

Fig. 5 demonstrates average diurnal profiles of O_3, NO_3^-, NH_3, HNO_3, and NO_2 for each season at Shanghai from CMAQ base simulation. In spring (MAM) as shown in Fig. 5(a), O_3 concentration started to increase from about 6:00 which is the local sunrise time, and started to decrease around 14:00. During this time period, NO_3^- was increasing slowly and both NO_2 and NH_3 were found decreased correspondingly. The negative correlation between NO_2 and NO_3^- within this episode indicated that, although HNO_3 daytime production was fast due to higher O_3 concentration, the formation of NO_3^- was not promoted significantly, which was probably caused by higher temperature that favors partition of particle phase NH_4NO_3. While O_3 and HNO_3 concentrations fall to bottom values around 22:00, NO_3^- kept increasing gradually. Meanwhile NO_2 also increased rapidly with a rising rate even larger than increasing of NO_3^-, indicating that formation of NO_3^- was mainly driven by the daytime accumulated HNO_3 before 22:00, since concentration of HNO_3 decreased rapidly and stayed low until the next morning. Enhancement of nitrate became increasingly fast after 0:00 with a sharp decrease of both NO_2 and NH_3, which apparently indicated that hydrolysis of N_2O_5 took over the primary role as NO_3^- producer from 0:00 to 6:00. Similar nighttime enhancement of NO_3^- was also found for other seasons as shown in Fig. 5(b)–(d). The diurnal variations of other species may change slightly between different seasons, but accumulation of NO_3^- was identified throughout the year. In addition, although nighttime lower PBL may also contribute to the higher concentration of NO_3^-, the simultaneously increase of NO_3^- and decrease of NH_3 between 0:00 and 4:00 suggested that the nocturnal production process plays the key role in determining the accumulation of NO_3^-.

It is also important to notice that nocturnal production of NO_3^- is greatly dependent on concentration of O_3 which is involved in reactions (R3) and (R4). Since O_3 could only be produced through photolysis reactions, the daytime accumulation of O_3 had substantial impact on the nighttime formation of NO_3^- as the major oxidant. While O_3 concentration is also closely determined by NOx, NO_3^- response under NOx emission change become more complicated, as discussed in next section.

3.3. Inorganic aerosols responses to NOx and VOC emission reductions

As the major precursor for both NO_3^- and O_3, a few studies already demonstrated that NOx emission change over YRD would lead to increase of O_3 especially in winter due to the local VOC-sensitive condition (Fu et al., 2012a; Dong et al., 2013). However, impact of NOx emission change on NO_3^- may retain many uncertainties due to the complicacy within the chemical processes discussed in last section. Under NOx emission reduction, although the daytime formation of HNO_3 might be directly slow down, less titration effect on the other hand will probably lead to higher accumulated O_3 and thus indirectly speed up the formation of NO_3^- through the nocturnal production pathway. Change of NH_4^+ is also unclear without modeling because it is dependent on changes of NO_3^- since YRD was NH_3-rich. Response of SO_4^{2-} is relatively more predictable since oxidization of SO_2 is mainly driven by hydroxyl radical, so SO_4^{2-} production may remain mostly unaffected. But the thermodynamic equilibrium of NO_3^-–SO_4^{2-}–NH_4^+ system will also be affected once NO_3^- concentration changes. Consequently, we examined the NO_3^-, SO_4^{2-}, and NH_4^+ responses to anthropogenic NOx and VOC emission changes in this section based on modeling results from control scenarios to reveal the inorganic aerosols sensitivity over YRD.

Fig. 6 described the seasonal average responses of inorganic aerosols under emission control scenarios P-N85 and I-V20. Usually with NOx emission reduction, NO_3^- was expected to decrease and SO_4^{2-} was expected to increase. However, under P-N85 scenario, we find increase of NO_3^- was found over east and north part of YRD in winter (DJF) with largest increment as 0.4 μg/m^3 in Shanghai, and decrease of NO_3^- was found over most part of YRD with up to 2.5 μg/m^3 in fall (SON). Simulated NH_4^+ in P-N85 showed weak response to NOx emission change, its concentration decreased slightly in spring (MAM), yet increased during summer (JJA), fall, and winter mainly over east part of YRD, with the largest increase as 0.2 μg/m^3 in winter over Shanghai. Changes of SO_4^{2-} were found to be positive for all seasons over the domain, with the largest increase up to 0.6 μg/m^3 in fall over Suzhou (~100 km northwestward of Shanghai). VOC emission change scenario I-V20 was found to have very weak impacts on inorganic aerosols as shown in Fig. 6, since it only directly affect O_3 chemistry. As majority of YRD is VOC-sensitive for O_3, concentration of NO_3^- was also found decrease slightly due to less oxidants available for both daytime and nighttime pathways under VOC reduction.

Fig. 7 describes seasonal average responses of NO_3^- under T-N20, I-N20 and T-V20 scenarios. The impacts of emission controls are similar between T-N20, I-N20 and P-N85, except that nitrate changes in smaller scale. This is consistent with expectation since less NOx emission is reduced in T-N20 and I-N20 as compared with P-N85 as mentioned in Section 2, while it also indicated that the nitrate responses (both increasing and decreasing) might be linear due to emission change. While 20% of VOC emission from industry seems not significantly affect the aerosols responses as shown in Fig. 6 for I-V20, same reduction ratio for T-V20 is demonstrated to reduce NO_3^- up to 0.18 μg/m^3 over YRD in winter. The difference between I-V20 and T-V20 indicated that reduction in transportation sector can effectively reduce the daytime production of O_3 and thus prohibit the formation of NO_3^- through daytime production.

The seasonal and spatial variations of aerosols response to NOx emission control indicated that both meteorology condition and emission intensity may lead to different sensitivity of NO_3^- over YRD, which will further affect the changes of NH_4^+ and SO_4^{2-}. In addition, O_3 sensitivity may have a significant impact on NO_3^- sensitivity in YRD. In order to better understand the temporal and spatial variations of NO_3^- sensitivity, monthly average diurnal profiles of O_3 and N_2O_5 were investigated. July and December were selected as the representative months to reveal the impact caused by different meteorology. Two 5 × 5 grid subsections were selected as one in Shanghai urban area and the other in Hangzhou rural area, to examine the different impacts caused by emission intensity.

Fig. 8 described O_3 and N_2O_5 responses under P-N85 and I-V20 scenarios over urban and rural sites in July and January. In July at urban site, daytime production of O_3 under I-V20 was found almost overlay with base case, indicating the rapid summer time photolysis production of O_3 was hardly affected by 20% VOC reduction from industry source over YRD. Although urban area in YRD was reported as VOC-sensitive condition (Li et al., 2011; Xing et al., 2011), industry VOC emission sources such as oil and chemical productions were mainly located in suburban area where NOx emission is low. Thus 20% control was insufficient to effectively reduce O_3 (T-V20 scenario with 20% VOC emission reduction from transportation does show a slight reducing impact on NO_3^- in winter due to decreased O_3, which is shown in Fig. 7). Under P-85 case, O_3 was higher than base case between 6:00 and 11:00, lower between 11:00 and 15:00, and almost same as base case between 15:00 and 23:00, suggesting that summer urban area in YRD was VOC-sensitive in daytime. Although both O_3 and N_2O_5 concentrations were slightly higher in P-N85 scenario between 0:00 and 05:00 due to less titration by lower NOx emission, N_2O_5 concentration between 10:00 and 23:00 was lower than base case, which resulted in the overall lower production of NO_3^- in summer over YRD as shown in Fig. 6.

While NOx reduction resulted in NO_3^- decrease in summer time, P-N85 was found having different impact in December. As shown in Fig. 8(b), in December, O_3 concentration increased by up to 11.8 ppbv

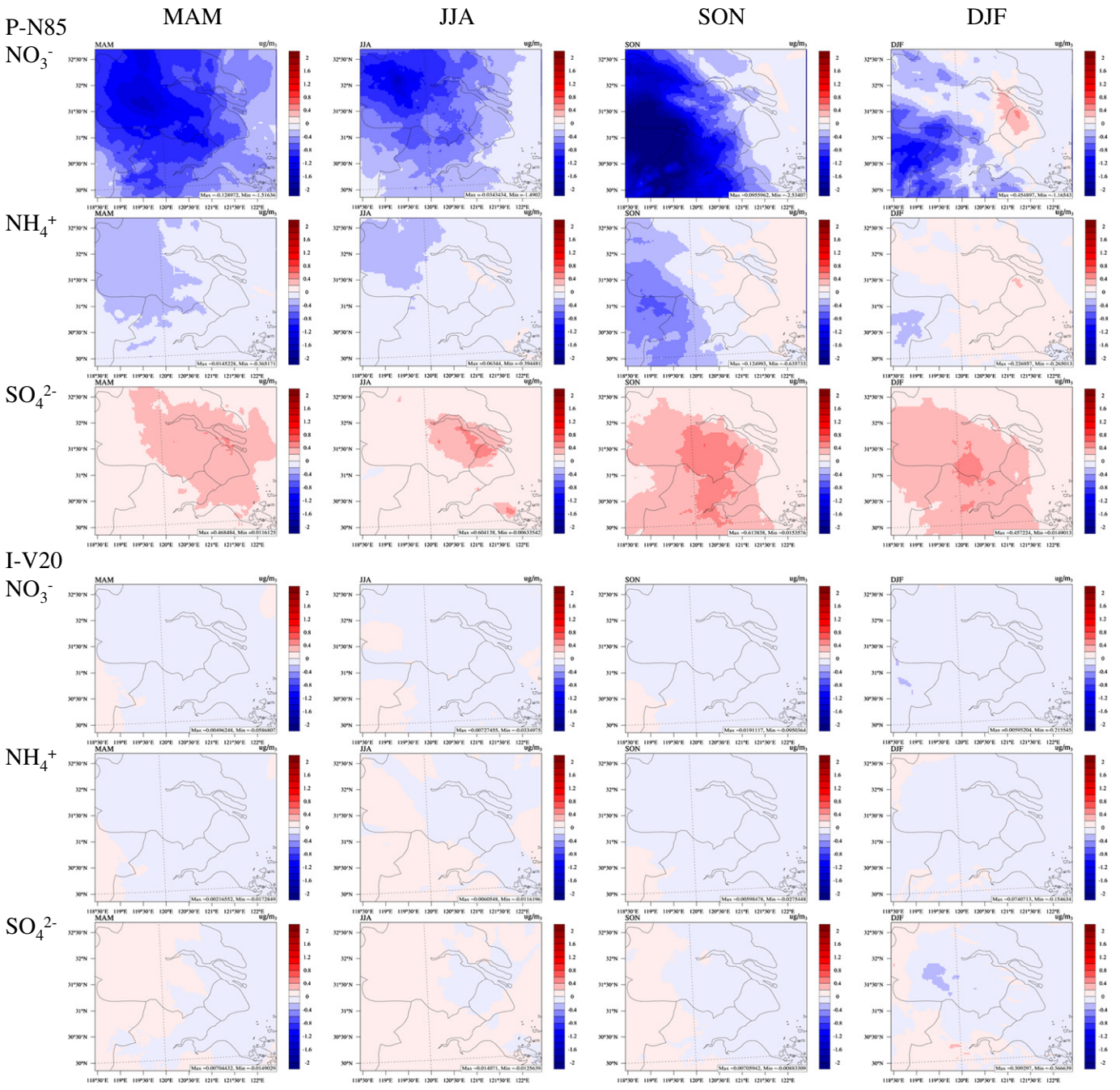

Fig. 6. NO_3^-, NH_4^+, and SO_4^{2-} responses under P-N85 (upper panel) and I-V20 (lower panel) scenarios in four seasons, blues indicate concentrations decrease and reds indicate increase.

(49% higher than base case) at 15:00 and up to 11.7 ppbv (78%) at 3:00 under the P-N85 scenario over the urban site, indicating that titration effect was strongly restrained under NOx emission reduction. Correspondingly, increase of O_3 lead to enhancement of N_2O_5 which mainly happened after 18:00 and before 5:00, with largest rise up to 0.22 ppbv (58%) at 2:00. While the difference of N_2O_5 between base and P-N85 was obviously much smaller during daytime, the large discrepancy during nighttime suggesting that NOx emission reduction over the urban site lead to rapid nocturnal formation of N_2O_5 due to excessive O_3 accumulated during daytime. So hydrolysis of N_2O_5 will then result in higher production of HNO_3 and NO_3^- under the NH_3-rich condition over YRD, and further lead to more formation of SO_4^{2-} and NH_4^+. This process explained the increase of inorganic aerosols over Shanghai during winter as shown in Fig. 6. VOC emission reduction also showed larger impact in December, as in I-V20 scenario O_3 concentration was decreased by up to 1.3 ppbv (10%) at 2:00, along with N_2O_5 concentration decreased by up to 0.017 ppbv (12%) at the same time. This negative response of O_3 and N_2O_5 implied the VOC-sensitive condition for both O_3 and NO_3^- during winter time over urban areas of YRD.

Fig. 8(c)–(d) described chemical responses over the rural site in two different seasons. Apparently, emission changes of VOC or NOx were found hardly to affect O_3 in July. N_2O_5 concentration was reduced slightly during nighttime under P-N85 scenario due to less NO_2 available.

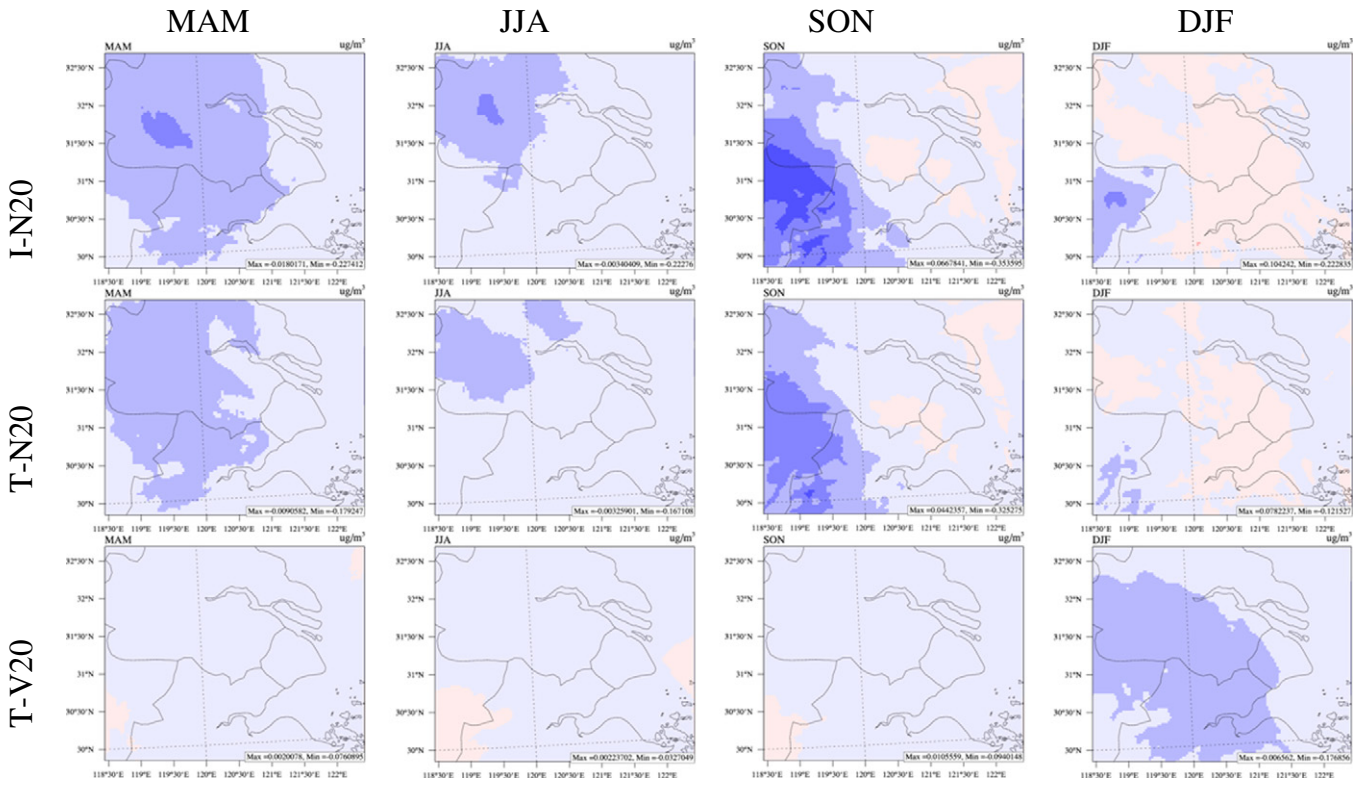

Fig. 7. Seasonal average of NO_3^- responses to I-N20 (upper panel), T-N20 (middle panel), and T-V20 (lower panel) scenarios.

Emission changes in December showed larger responses as O_3 increased slightly during daytime, and N_2O_5 was reduced greatly during nighttime under P-N85 scenario, while I-V20 showed adverse effect but within much smaller scale. This result indicated that rural area over YRD might be slightly VOC-limited for O_3, but reduction of NOx emission may still lead to decreasing of NO_3^-.

4. Conclusion

In-situ observations of fine particles, satellite observations and the MM5/CMAQ modeling system were used to examine the $PM_{2.5}$ pollution over Yangtze River Delta area in China. $PM_{2.5}$ pollution was found in severe status by evaluating its ambient concentration

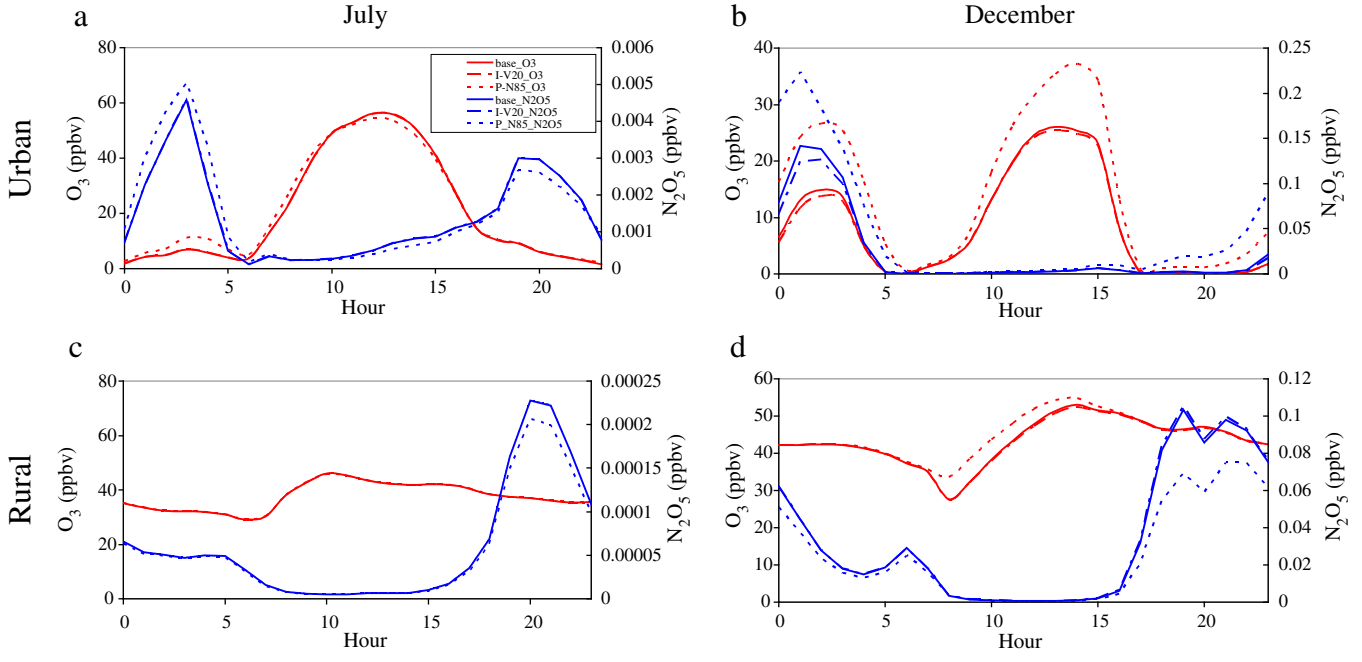

Fig. 8. Monthly average diurnal profiles of O_3 (red lines) and N_2O_5 (blue lines) in July (left column, (a) and (c)) and December (right column (b) and (d)) from urban (upper row) and rural (lower row) area. Cases shown here include base case (solid lines), I-V20 (alternating long and short dashed line), and P-N85 (dash lines).

against the new published China National Ambient Air Quality Standard, with 58% of the research domain exceeding the annual standard. $PM_{2.5}$ was also found to have a strong seasonality which was affected by significant contributions from inorganic aerosols. Total NO_3^-, SO_4^{2-}, and NH_4^+ contributed to 36%–49% for $PM_{2.5}$ mass over YRD, generally with higher concentrations in winter and lower values in summer.

In order to understand the contributions from inorganic aerosols, especially the high NO_3^- over YRD, diurnal variation analysis was performed to examine the chemical production process of NO_3^-. The results suggested that nocturnal production may be responsible for the high NO_3^- concentration in NH_3-rich condition over YRD. While other studies suggested this process may be only obvious in certain episodes, our results demonstrated that nighttime enhancement of NO_3^- may have important impact on inorganic aerosol formation throughout the year, although the effect was especially significant in winter due to favored condition for hydrolysis of N_2O_5.

Sensitivity responses of inorganic aerosols were also analyzed in order to provide fundamental information for potential emission control activity aiming at reducing PM pollution over YRD. We find that simply reducing NOx emission will lead to increase of NO_3^- in winter over the urban areas, although NO_3^- will be decreased for other seasons and areas. Changes of NO_3^- is also found to affect the responses of other inorganic aerosols, where NH_4^+ might be slightly increase or decrease depending on time and location, and SO_4^{2-} was found mostly increase moderately under NOx emission control. On the other hand, VOC emission control was found reduce NO_3^- concentration especially in winter, although it is not directly related to formation. It turns out NO_3^- formation is restrained through the nocturnal production process because YRD is VOC-limited for O_3 production, and reducing VOC would lead to less O_3 and thus slow down the production of N_2O_5 during nighttime. Since NOx emission reduction has been included in the national 12th-five-year-plan (12th FYP), our findings in this study suggested that a multi-pollutant reduction strategy that integrates control measures to reduce both NOx and VOC should be indeed more effective.

Moreover, while different reduction ratios were applied in this study, it should be noticed that nitrate response to NOx emission change is possibly nonlinear although we do see the consistency between I-N20/T-N20 and P-N85 scenario. Future work should extend this sensitivity modeling analysis by applying more reduction/increase ratios such as response surface modeling (Xing et al., 2011) to explicitly examine the inorganic aerosols responses.

Conflict of interest

The results presented here are the views of the authors and not the official views of the CDC and the US Department of Energy — ORNL.

Acknowledgment

This study was supported by the Energy Foundation under Grant No. G-1208-16611. This work was also partially support by the National Key Project of Basic Research of China (Grant No. 2006CB403704) and the National Natural Science Foundation of China (Grant Nos. 20877020, 40575062, and 40599420) of China. Yang Gao is partly supported by the Office of Science of the U.S. Department of Energy as part of the Regional and Global Climate Modeling Program. The Pacific Northwest National Laboratory is operated for DOE by Battelle Memorial Institute under contract DE-AC05-76RL01830. Any opinions, findings, and conclusions expressed in this material are those of the authors.

Appendix A. Supplementary data

Supplementary data to this article can be found online at http://dx.doi.org/10.1016/j.scitotenv.2014.02.076.

References

Ansari AS, Pandis SN. Response of inorganic PM to precursor concentrations. Environ Sci Technol 1998;32:2706–14.
Babich P, Davey M, Allen G, Koutrakis P. Method comparisons for particulate nitrate, elemental carbon, and $PM_{2.5}$ mass in seven US cities. J Air Waste Manage Assoc 2000;50:1095–105.
Byun D, Schere KL. Review of the governing equations, computational algorithms, and other components of the models-3 Community Multiscale Air Quality (CMAQ) modeling system. Appl Mech Rev 2006;59:51–77.
Chan CK, Yao X. Air pollution in mega cities in China. Atmos Environ 2008;42:1–42.
China National Environmental Monitoring Centre Centre. Monthly air quality reports over 74 cities. Available athttp://www.cnemc.cn/publish/totalWebSite/0666/newList_1.html, 2013. [in Chinese].
Dong XY, Gao Y, Fu JS, Li J, Huang K, Guoshun Z. Probe into gaseous pollution and assessment of air quality benefit under sector dependent emission control strategies over megacities in Yangtze River Delta China. Atmos Environ 2013;79:841–52.
Du Y. New consolidation of emission and processing for air quality modeling assessment in Asia [M.S. Thesis] University of TennesseeKnoxville, TN: University of Tennessee; 2008 [76 pp.].
EPA. Guidance on the use of models and other analyses for demonstrating attainment of air quality goals for ozone, $PM_{2.5}$ and regional haze; 2007.
Fu QY, Zhuang GS, Li JA, Huang K, Wang QZ, Zhang R, et al. Source, long-range transport, and characteristics of a heavy dust pollution event in Shanghai. J Geophys Res Atmos 2010;115. http://dx.doi.org/10.1029/2009JD013208.
Fu JS, Dong XY, Gao Y, Wong DC, Lam YF. Sensitivity and linearity analysis of ozone in East Asia: the effects of domestic emission and intercontinental transport. J Air Waste Manage Assoc 2012a:62.
Fu JS, Hsu NC, Gao Y, Huang K, Li C, Lin NH, et al. Evaluating the influences of biomass burning during 2006 BASE-ASIA: a regional chemical transport modeling. Atmos Chem Phys 2012b;12:3837–55. http://dx.doi.org/10.5194/acp-12-3837-2012.
Fu X, Wang SX, Zhao B, Xing J, Cheng Z, Liu H, et al. Emission inventory of primary pollutants and chemical speciation in 2010 for the Yangtze River Delta region, China. Atmos Environ 2013;70:39–50.
Guenther AB, Jiang X, Heald CL, Sakulyanontvittaya T, Duhl T, Emmons LK, et al. The Model of Emissions of Gases and Aerosols from Nature version 2.1 (MEGAN2.1): an extended and updated framework for modeling biogenic emissions. Geosci Model Dev 2012;5:1471–92. http://dx.doi.org/10.5194/gmd-5-1471-2012.
Huang K, Zhuang G, Lin Y, Fu JS, Wang Q, Liu T, et al. Typical types and formation mechanisms of haze in an Eastern Asia megacity, Shanghai. Atmos Chem Phys 2012;12:105–24. http://dx.doi.org/10.5194/acp-12-105-2012.
Krotkov NA, McClure B, Dickerson RR, Carn SA, Li C, Bhartia PK, et al. Validation of SO_2 retrievals from the ozone monitoring instrument over NE China. J Geophys Res Atmos 2008;113. http://dx.doi.org/10.1029/2007JD008818.
Lam YF, Fu JS. A novel downscaling technique for the linkage of global and regional air quality modeling. Atmos Chem Phys 2009;9:9169–85. http://dx.doi.org/10.5194/acp-9-9169-2009.
Li L, Chen CH, Huang C, Huang HY, Zhang GF, Wang YJ, et al. Ozone sensitivity analysis with the MM5-CMAQ modeling system for Shanghai. J Environ Sci China 2011;23:1150–7.
Malm WC, Schichtel BA, Pitchford ML, Ashbaugh LL, Eldred RA. Spatial and monthly trends in speciated fine particle concentration in the United States. J Geophys Res Atmos 2004;109. http://dx.doi.org/10.1029/2003JD003739.
Pathak RK, Wang T, Wu WS. Nighttime enhancement of $PM_{2.5}$ nitrate in ammonia-poor atmospheric conditions in Beijing and Shanghai: plausible contributions of heterogeneous hydrolysis of N_2O_5 and HNO_3 partitioning. Atmos Environ 2011;45:1183–91.
Pinder RW, Dennis RL, Bhave PV. Observable indicators of the sensitivity of $PM_{2.5}$ nitrate to emission reductions — part I: derivation of the adjusted gas ratio and applicability at regulatory-relevant time scales. Atmos Environ 2008;42:1275–86.
Pun BK, Seigneur C. Sensitivity of particulate matter nitrate formation to precursor emissions in the California San Joaquin Valley. Environ Sci Technol 2001;35:2979–87.
Streets DG, Fu JS, Jang CJ, Hao JM, He KB, Tang XY, et al. Air quality during the 2008 Beijing Olympic Games. Atmos Environ 2007;41:480–92.
Wang SX, Xing J, Jang CR, Zhu Y, Fu JS, Hao JM. Impact assessment of ammonia emissions on inorganic aerosols in East China using response surface modeling technique. Environ Sci Technol 2011;45:9293–300.
Wang SX, Xing J, Zhao B, Jang C, Hao JM. Effectiveness of national air pollution control policies on the air quality in metropolitan areas of China. J Environ Sci 2014;26:13–22.
Xing J, Wang SX, Jang C, Zhu Y, Hao JM. Nonlinear response of ozone to precursor emission changes in China: a modeling study using response surface methodology. Atmos Chem Phys 2011;11:5027–44. http://dx.doi.org/10.5194/acp-11-5027-2011.
Yarwood G, Rao S, Yocke M, Whitten G. Updates to the carbon bond chemical mechanism: CB05. Final report to the US EPA, RT-0400675; 2005 [available at http://www.camx.com/publ/pdfs/cb05_final_report_120805.pdf].

Zhang Q, Streets DG, Carmichael GR, He KB, Huo H, Kannari A, et al. Asian emissions in 2006 for the NASA INTEX-B mission. Atmos Chem Phys 2009;9:5131–53. http://dx.doi.org/10.5194/acp-9-5131-2009.

Zhang XY, Wang YQ, Niu T, Zhang XC, Gong SL, Zhang YM, et al. Atmospheric aerosol compositions in China: spatial/temporal variability, chemical signature, regional haze distribution and comparisons with global aerosols. Atmos Chem Phys 2012;12:779–99.

Zhao Y, Wang SX, Duan L, Lei Y, Cao PF, Hao JM. Primary air pollutant emissions of coal-fired power plants in China: current status and future prediction. Atmos Environ 2008;42:8442–52.

Zhao B, Wang SX, Wang JD, Fu JS, Liu TH, Xu JY, et al. Impact of national NOx and SO_2 control policies on particulate matter pollution in China. Atmos Environ 2013a;77:453–63.

Zhao B, Wang SX, Dong XY, Wang JD, Duan L, Fu X, et al. Environmental effects of the recent emission changes in China: implications for particulate matter pollution and soil acidification. Environ Res Lett 2013b;8:024031.